Plasma Polymerisation of (2,2,6,6-Tetramethylpiperidin-1-yl)oxyl (TEMPO) in a Collisional, Capacitively-coupled Radio Frequency Discharge

Running title: Plasma Polymerisation of TEMPO

Running Authors: Barnes et. al.

Michael J. Barnes

Department of Electrical Engineering and Electronics, University of Liverpool, Brownlow Hill, L69 3GJ, Liverpool, UK

Alexander J. Robson

Department of Chemistry/Material Science Institute, University of Lancaster, Bailrigg, LA1 4YW, Lancaster, UK

Javad Naderi

Department of Chemistry/Material Science Institute, University of Lancaster, Bailrigg, LA1 4YW, Lancaster, UK

Robert D. Short

Department of Chemistry/Material Science Institute, University of Lancaster, Bailrigg, LA1 4YW, Lancaster, UK

James W. Bradley [a)]

Department of Electrical Engineering and Electronics, University of Liverpool, Brownlow Hill, L69 3GJ, Liverpool, UK

[a)]Electronic mail: jbradley@liverpool.ac.uk

Plasma polymerisation of TEMPO (2,2,6,6-Tetramethylpiperidin-1-yl)oxyl yields thin films containing stable nitroxide radicals which have properties analogous to that of NO without short lifetimes. This property gives TEMPO films a wide variety of potential applications. Typically control of the final film chemistry is difficult and the plasma

discharge conditions must be tailored to in order to maximise the retention of these nitroxide groups during the polymerisation and deposition process. In this study, plasma diagnostics and surface analysis of the deposited films were carried out to determine the optimal plasma conditions for the retention of nitroxide groups. These techniques included energy-resolved mass spectrometry, heated planar probe ion current measurements, deposition rate measurements, and X-ray photoelectron spectroscopy. Results show that operating the plasma with a combination low input powers and high pressures leads to a collisional discharge in which fragmentation of the TEMPO molecule is suppressed, leading to good retention of nitroxide groups. IEDFs and QCM measurements support the soft landing theory of ion deposition on the substrate within this γ-mode, in which the flux of low energy, soft landed ions form the primary contribution to film growth. XPS analysis of deposited polymers shows 75.7% retention of N-O groups in the polymer films deposited in a 25 Pa 5 W discharge.

I. INTRODUCTION

Plasma polymerisation is a technique used for the deposition of ultrathin functionalised films onto surfaces. It is a single step process, independent of the substrate, does not require the use of solvents and can be used to tailor the surface chemistry without altering the bulk properties of the material. [1] The ability of the plasma polymerisation process to homogeneously coat numerous materials makes it useful for a wide range of applications such as grafting cells or proteins onto surfaces[2,3] , modifying the hydrophilic/hydrophobic properties of materials[4], and the development of antifouling

surfaces.[5] Functional groups which have commonly been deposited in plasma polymers include amines and amides[6,7], carboxyls[8], hydroxyls[9,10], and aldehydes.[11]

Studies using DC[12,13] and microwave[14] plasma polymerisation have been reported, but the majority of experiments have used RF plasmas. Usually a low pressure environment is used for the deposition of these polymer films, in which the mean-free-paths of ionic and neutral molecular species is large relative to the vacuum chamber dimensions. The discharge will contain numerous different chemical species and oligomers and the final film chemistry is difficult to control, often sharing little similarities with the precursor molecule. Techniques which have been utilised in order to gain greater control of the surface functionalisation include reduced plasma power [7,15] or pulsing the power [16,17,18,19] to produce a greater surface density of the desired functional group. In either case, simplistically the power monomer unit is lower.

Higher pressure discharges have also been used to retain the starting compound ("monomer") chemistry to the deposit.[20] Higher pressure results in a shift from a discharge operating in from the α-mode where the sheaths are broadly collisionless to the collisional γ-mode. Previously it has been shown that operation in collisional γ-mode results in a substantial flux of protonated monomer ion to immersed surfaces within the plasma.[5]

From previous studies of plasma polymerisation a working hypothesis is formulated and tested herein: the retention of a fragile or complex chemical moiety is first favoured by

the use of low plasma power, but that further advantage is also gained from the additional use of higher plasma pressures. Low power reduces the degree of plasma-phase fragmentation and the plasma sheath potentials, whilst on moving into the collisional γ-mode, sheath potentials collapse further, and protonation of intact monomer will occur within the sheath region and account for polymer formation. The combination of low power and high pressure may result in greater functional retention than that observed using reduced power or higher pressure alone.

(2,2,6,6-Tetramethylpiperidin-1-yl)oxyl (TEMPO) was chosen as the monomer as a recent report was published showing the use of TEMPO to produce plasma polymers with high concentrations of nitroxide groups. Nitric oxide (NO) is an important signalling molecule in many biological processes. It has been demonstrated that NO can be utilised in applications ranging from biofilm dispersal [21], to the treatment of certain cancer types [22], and the modification of stem cell behaviour.[23] However NO has a short lifetime due to its reactive properties, which has led to interest in stable radicals with similar properties such as TEMPO, an organic molecule containing a stable nitroxide radical. These nitroxide groups have properties analogous to NO without the detrimentally short lifetime and recent work has shown that TEMPO plasma polymers can inhibit the formation of biofilms by the bacteria *Staphylococcus epidermidis* and *Candida albicans* and modulate inflammation. [24, 25]

Whilst carrying out the work presented here, a mass spectrometric study of the ionic TEMPO plasma species was reported [26] across the pressure range of 1-6 Pa with a fixed

plasma input power, as well as an analysis of the resultant polymer films using a combination of electron spin resonance, time of flight ion mass spectrometry, and liquid chromatography mass spectrometry. Therefore the aim of this work is to advance that previously undertaken and present a detailed diagnostic study of an RF, capacitively coupled TEMPO plasma across a broad range of operational pressures (5-25 Pa) and powers (5-30 W). This was performed using in-situ mass spectrometry for the ionic and neutral plasma species, heated planar probe for determination of the arriving ion fluxes (saturation currents), quartz crystal microbalance, and an analysis of plasma polymer coatings by X-ray photoelectron spectroscopy. It is worth noting that the results presented here cannot be generalised for all vacuum vessels, for example the reactor used here has a different shape and electrode configuration compared to [26], which will not likely result in identical TEMPO polymer films. [27]

II. EXPERIMENTAL SET UP AND METHODOLOGY

A. Vacuum Chamber

All measurements and plasma polymer film depositions were performed in a QVF glass cruciform vessel with a volume of approximately 7000 cm^3, shown in figure 1 a). The chamber was evacuated using an Edwards E2M2 two stage pump and Edwards EXT70 turbomolecular pump in order to achieve a base pressure of $1x10^{-2}$ Pa. The operating pressure of the system was adjusted using a combination of the precursor flow rate and a gate valve situated in front of the turbo pump, monitored using an Edwards APG Pirani pressure gauge. An in-line liquid nitrogen cold trap was placed in front of the

turbomolecular pump in order to capture TEMPO vapour as it is removed from the chamber to protect the pumping system. A Coaxial Power Systems RFG 150 was used to deliver continuous wave 13.56 MHz RF power to a two-turn unterminated coil to ignite a capacitively coupled plasma discharge. The chamber end plates and the body of the mass spectrometer acted as the grounded electrodes. As the powered electrode is coiled around the vessel, the distance between the electrodes varies from around 3cm to 15cm depending on the location in the vacuum chamber.

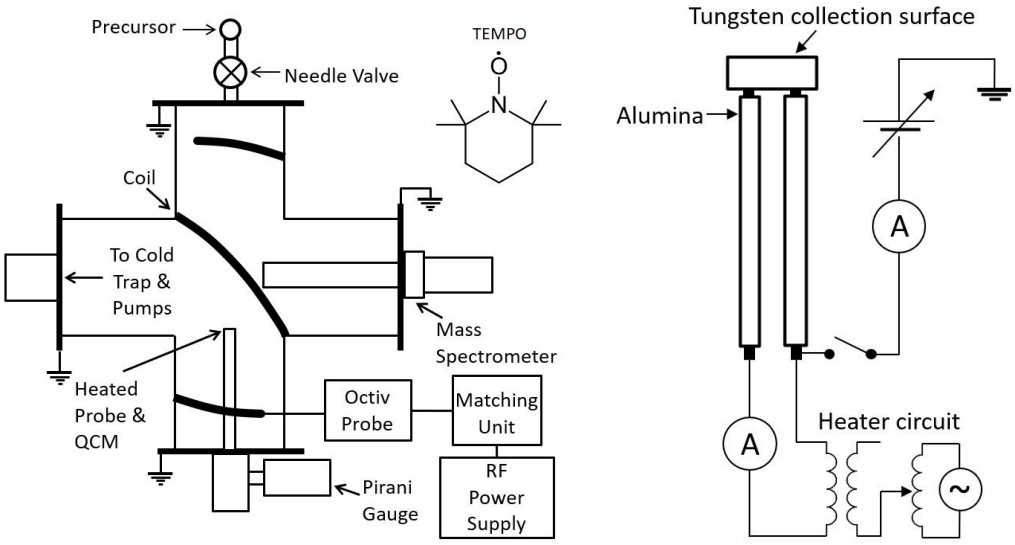

FIG. 1. a) Diagram of the vacuum chamber and apparatus, and b) Design of the planar heated probe used for ion current measurements.

TEMPO (98 %+) was purchased from Fisher Scientific and used without any further purification. As the TEMPO sublimated it was kept in a bath of room temperature water to maintain a constant temperature as vapours flowed into the chamber. The monomer flow rate was adjusted to achieve the desired pressure, but was not explicitly measured. TEMPO plasma discharges were investigated across a pressure range of 5-25 Pa (3.7 x10^{-}

^{2} -1.9 x 10^{-1} Torr), with input RF powers varying from 5-30 W. Plasma polymer deposition times were twenty minutes for all discharge conditions.

Measurement of the RF current-voltage characteristics and power delivered to the unterminated coil was conducted using an Impedans Octiv poly current voltage probe. The probe was placed as close to the powered electrode as possible. All the results presented refer to the IV characteristics of the fundamental RF frequency and all powers referred to in the rest of this work are those measured by the Octiv current voltage system.

B. Plasma Mass Spectrometry

Plasma mass spectrometry was carried out using a HIDEN Analytical EQP 300 mass-energy analyser for in-situ measurements mass spectrometry of neutral and positive ion species, as well as ion energy distributions (IEDFs). The mass and energy resolutions were 0.1 amu and 0.1 eV respectively. The aperture of the spectrometer was positioned approximately 25 mm from the centre of the vacuum vessel. When operated for analysis of positive ion species the spectrometer was tuned for the maximum intensity of the energy distribution of ions at 126 amu, as this was typically the largest peak present in the spectra.

Analysis of plasma phase neutral species was carried out inside the mass spectrometer using an internal electron impact (EI) source. This source had an electron accelerating potential set to 70 V with a current of 100 μA. The energy of the electrons within the EI

source (70 eV) is sufficient to dissociate neutral molecules entering the spectrometer. EI results in significant fragmentation of neutrals. EI spectra collected from plasma-phase neutrals have been corrected using an EI spectrum obtained from the intact TEMPO molecule (plus any impurities present in the vacuum chamber) which is shown in figure 2. This spectrum is used to correct all peaks in the spectrum, excluding the representing the TEMPO molecule, via a cracking analysis by applying Eq. (1) (outlined in [16]) to

$$I_c(m) = I_m(PlasmaON) - \left(I_m(PlasmaOFF) \times \frac{I_{prec}(PlasmaON)}{I_{prec}(PlasmaOFF)}\right) \qquad (1)$$

where $I_c(m)$ is the corrected peak intensity for a molecule mass m, I_m is the uncorrected intensity, and I_{prec} is the precursor peak intensity. Neutral and ion spectra were also corrected to take the transmission of the spectrometer into account, which is proportional to approximately m^{-1} according to documentation from Hiden Analytical. Peaks were also normalised to the total count before analysis for all mass spectra and IEDFs.

C. Deposition Rate Measurements

A Maxtek TM-400 multi-film deposition monitor quartz crystal microbalance (QCM) was used to measure the deposition rate of the TEMPO plasma across the operating conditions investigated. Typically, the rate measured by the QCM stabilised after a few seconds once the plasma had been ignited. The deposition rate recorded with no plasma was less than 0.1 Å/s for all pressures. Aluminium substrates were initially cleaned with acetone before TEMPO plasma polymers (TEMPOpp) were deposited for

20 minutes at each respective pressure/power. The changing quartz resonant frequency is converted into a changing thickness using Eq.2

$$TK_f = \left(\frac{P_q}{P_f}\right) N_q \left(\frac{t}{\pi R_z}\right) arctan\left[R_z tan\pi\left(\frac{t-t_g}{t}\right)\right] \qquad (2)$$

Where TK_f is the film thickness, P_q is the quartz density, P_f is the film density, N_q is a frequency constant for cut quartz, t is the period of the loaded crystal, t_q is the period of the unloaded crystal, and R_z is the acoustic impedance ratio of the loaded and unloaded crystal. The density of the film was estimated to the density of water, whilst the acoustic impedance of the plasma polymer was assumed to be the same as the impedance of quartz (i.e. $R_z = 1$). As the deposited polymer grows in thickness this assumption will become less valid and errors in the deposition rate increase, which can result in an uncertainty in the measured rate of around 20%.

D. Heated Planar Probe for Ion Saturation Currents

Due to the large number of different ionic species with varying mass, the large pressure range explored, changing degree of precursor dissociation with operational pressure/input power, and the presence of RF sheath oscillations, it is difficult to implement Langmuir probes in the TEMPO discharge. A heated planar electrical probe was used to estimate the ionic mass flux in the plasma volume by using the ion saturation current, as shown in figure 1 b). The probe was constructed from a double copper vacuum feed-through, with two alumina cylinders insulating the majority of the copper

surface. A small planar piece of tungsten was mounted onto the stem using two small springs attached to the ends of the copper rods. The surface area of the tungsten was 1.2 cm^{-2} with the rest of the probe surface covered in insulating tape to prevent drawing any extra current. The collection area was biased negatively from -20 V to -50 V to repel the electron population and collect an ion saturation current. Perturbation of the plasma should be minimal as the μA of ion current drawn is small relative to the current drawn by the chamber walls. Between each measurement, a secondary circuit was used to heat the probe to approximately 200 $^{\circ}$C with 1-1.2 A of current and remove any coatings that may have been deposited. The surface was allowed to cool for 90 s before starting the next measurement.

E. X-ray Photoelectron Spectroscopy

X-ray photoelectron spectroscopy (XPS) was performed on plasma polymers using a Kratos Analytical AXIS Supra spectrometer. Chemical analysis of the films was made using monochromatic Al Kα 1486.7 eV, operating at 15 kV, 15 mA, and equipped with an electron flood gun for charge neutralisation. All binding energies were referenced to the C1s peak at 285 eV in order to compensate for surface charging. The analysis area on each sample was 300x700 μm. Spectra were analysed using CasaXPS software (Casa Software Ltd, UK). Experimental sensitivity factors (N1s = 1.31, O1s = 0.59; C1s = 1) were determined using standard PET and polyamide (Nylon 6) polymers (818-277-81 and 694-8682-05, Goodfellow Cambridge Ltd, UK).

III. RESULTS AND DISCUSSION

A. Measurements of Ion Bombarding Flux

Characterisation of the TEMPO discharge was carried out using the heated planar probe and mass spectrometry of plasma species. Figure 2 shows the ion flux estimated using the ion saturation current collected by the heated electrical probe as the pressure and power were increased. Assuming every ion incident is singly ionised, the measured saturation current can be converted into an ion flux incident onto the planar surface using Eq. (3)

$$\varphi = \frac{I_{sat}}{eA} \qquad (3)$$

where A is the heated probe surface area, and e is the electron charge. As expected, the ion flux increases with RF power due to the larger plasma density surrounding the planar probe surface. Increasing pressure reduces the measured flux most likely due to the lower average energy per molecule, reducing fragmentation and the ion velocity as they approach the surface.

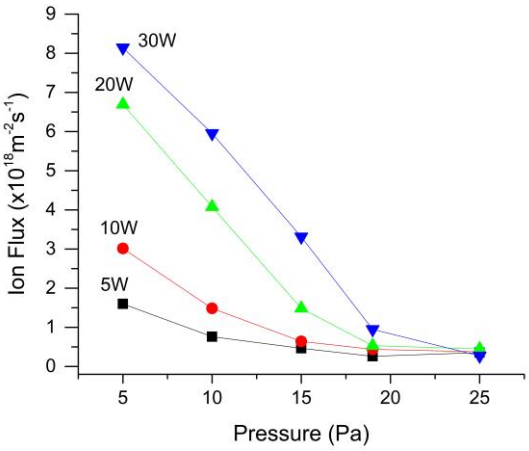

FIG. 2. The ion flux incident onto the planar probe surface calculated from the ion saturation current drawn by the probe when negatively biased.

Typically, as the plasma becomes increasingly collisional at higher pressures it may transition into the strong current regime, γ-mode, where the ionisation is dominated by secondary electron emission from surfaces. In this regime regions with the most intense ionisation will be situated close to substrates, which will likely affect the formation of polymer films on these surfaces.

B. Plasma Mass Spectrometry

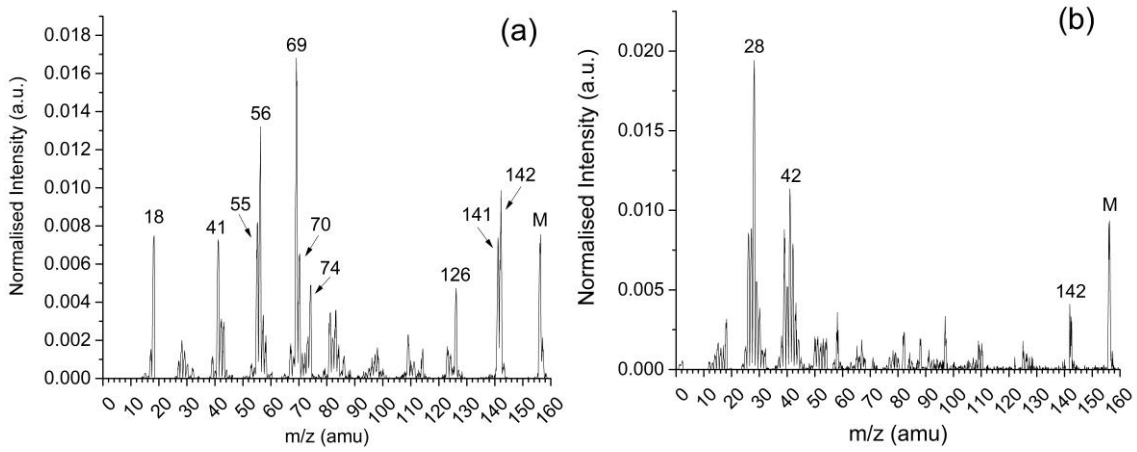

FIG. 3. a) Electron impact spectrum of TEMPO without a plasma at 15 Pa, and b) Neutral species measured from a 15 Pa 10 W plasma after correcting for fragmentation of the precursor by ionisation source electrons.

A previous study has investigated the mass spectrometry of piperidine nitroxides, including TEMPO.[28] Using this paper the following assignments can be made for figure 3 a). They acknowledge the challenge in m/z assignments that arises from TEMPO possessing an unpaired electron. This makes assigning the molecular ion at /z 156 more complicated, but they favour φ-N^+=O (φ = phenyl ring). They note the appearance of an ion at m/z 157 which corresponds to the free radical abstraction of H from water in the mass spectrometer. This ion decomposes by loss of a methyl group and explains the m/z 142 (through formally denoted $(M-14)^+$. (Methylene loss from m/z 156 is unlikely.). The m/z 126 has contributions from both $C_8H_{16}N$ and $C_7H_{12}NO$, but does not represent loss of NO. M/z 69 is given by C_5H_9 and they note that the series of even m/z ions at e.g. 74, 70, 56, etc. represent N-containing species; whilst those at odd m/z are more likely to be C-, H-, and C-, H-, and O-containing ions.

Figure 4 shows the typical corrected spectra observed for neutral species at 10 and 25 Pa. As the plasma transitions to the higher pressure regime (25Pa) the intact TEMPO monomer peak at 156 amu, labelled *M*, begins to dominate the spectrum.

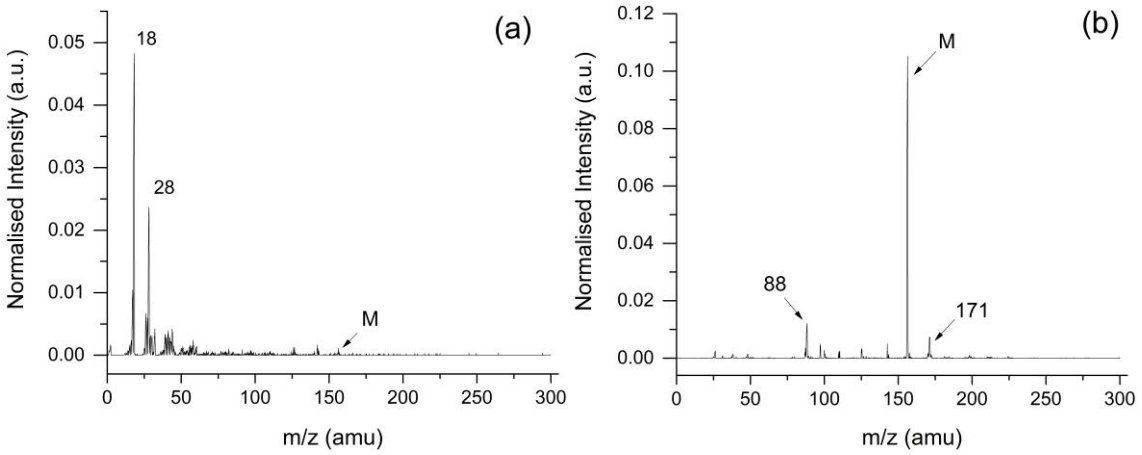

FIG. 4. Neutral species spectra for a) 10 Pa 30 W, and b) 25 Pa 5 W. Lower mass molecules form a more substantial fraction of the total signal in the spectrum at lower pressures and increased RF power due to fracturing of the TEMPO molecule.

As input power is increased, or operational pressure decreased, peaks from smaller molecules, fragments of the monomer arise and eventually begin to dominate the spectrum. With increased power there is a larger population of higher energy electrons and a greater plasma density leading to, the average electron impact imparting more energy and a higher frequency of electron-monomer collisions leading to greater molecular dissociation. In a similar effect, increasing the gas pressure will reduce the electron temperature and suppress the high energy electrons as the electron mean free path decreases. This will decrease monomer fragmentation as the average electron impact deposits less energy. This is consistent with the diminishing ion saturation currents with

increasing pressure as the smaller mean free path of electrons and ions in the plasma decreases their energy and flux.

The fragments at m/z 18 and 28 could represent H_2O^+ and $C_2H_4^+$, CO^+, CH_2N^+ and/or N_2^+; unfortunately, we do not have sufficient mass resolution to resolve, nor are they reported in Morrison and Adams. However, M/z 88 represents $C_4H_{10}NO$. [26] The neutral seen at m/z 171 is most interesting, it is not usual in plasma mass spectrometry of the neutrals to observe ions > *M*; the only previous case being in the plasma gas-phase reactions of alkyl methacrylates. [29]

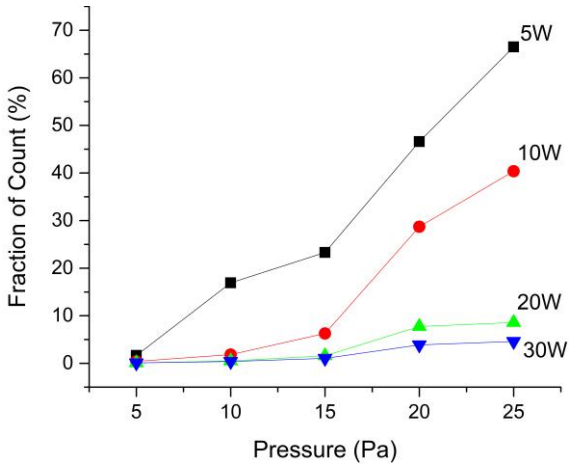

FIG. 5. Fraction of the total signal attributed to M, the intact TEMPO molecule, across the range of pressures and powers investigated.

Figure 5 shows the total count of the monomer *M* normalised to the total count of the whole spectrum. To maximise the number of molecules containing nitroxide groups in the pressure regime under investigation, a large flux of undissociated precursor molecules incident onto the substrate is sought. Figure 5 demonstrates that higher pressures and

lower input powers results in *M* forming an increasingly more substantial fraction of the incident neutral particle flux. Dependent on mode of film growth, abundant *M* has the potential to lead to greater retention of nitroxide groups in the resulting plasma polymers.

Figure 6 shows mass spectra of positive ions species collected from the discharge. Positive ions only make up a small fraction of the total particle number density inside the plasma bulk but are directionally accelerated across the plasma sheath. Consequently at surfaces they form a significantly larger fraction of the total incident particle flux.[30] An average ionic interaction with the substrate will impart significantly more energy than a neutral collision which means ions are potentially an important factor in thin film growth.

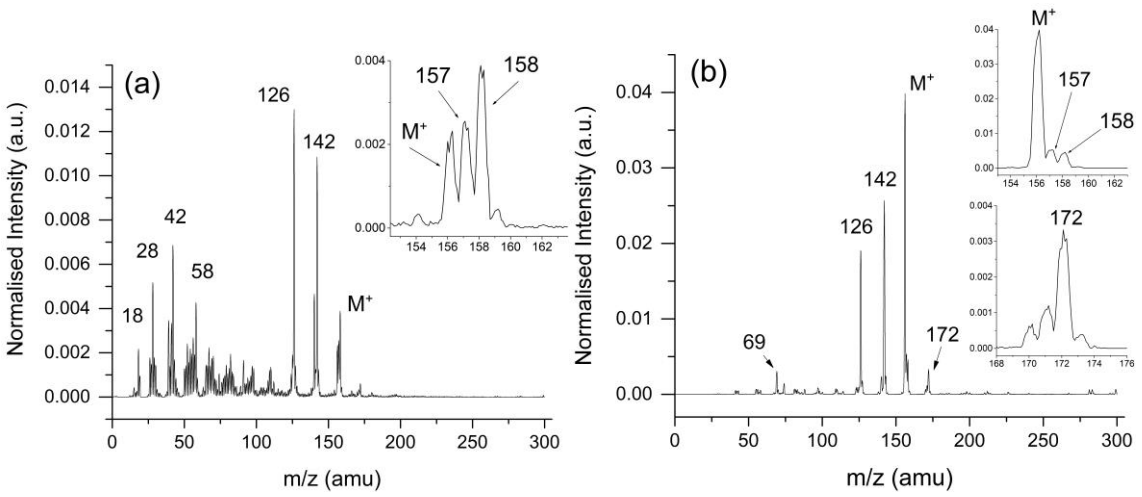

FIG. 6. Normalised mass spectra recorded for positive ions for a) 5 Pa 30 W, and b) 25 Pa 5 W. The sub figures show the peaks around M^+ in more detail.

In Figure 6 it can be seen that higher power and lower pressure favours *M* fragmentation (as was seen in the electron impact.). At high power and lower pressure, three ions are

seen at *M*, representing m/z 156= φ-N-O^+ (loss of an electron) m/z 157= NH^+-$O^{\cdot}$ (we postulate that protonation occurs on the N and *M* retains a radical on the oxygen) and m/z 158 = φ-NH^+-OH. This is an unusual observation, with a protonated radical cation molecule and a doubly protonated ion not having been seen previously in the positive ion mass spectrometry of plasmas of amines.[31] These possibilities arise from the complex electronic configuration of the nitroxide moiety.[28]

At higher pressure (lower power) m/z 156 > 157 and 158, and this ion at an even m/z is typical of a nitrogen-containing piperidine molecular ions. As previously discussed, other ions detected have already been identified (m/z 142, 126, 58, 42, etc). Unique to the higher pressure is m/z 69 assigned to $C_5H_9^+$. As a rule odd m/z positive ions correspond to C-, H- and C-, H- and O- containing ions.[32]

Morrison and Adams do not report any loss of NO at 70 eV for TEMPO and we do not see in the neutrals or positive ions any fragments that indicate NO loss (ie. m/z 30, 31). This is suggestive, but not conclusive of plasma phase retention of NO.

Results shown in figure 6 demonstrate that signals from smaller molecules are suppressed at higher pressure or lower power as fracturing of the precursor molecule is reduced. There is also some evidence of ions >*M* at m/z 270. This is likely due to dimerization but cannot be confirmed as they are situated outside the mass range of the spectrometer. The shift to higher m/z is reflected in the normalised total count of the ionised monomer M^+ across the investigated operational condition shown in figure 7. Similar trends are

observed to the neutral precursor signal in figure 5 with the relative fraction of the total signal corresponding to M^+ increasing as the power is reduced or pressure increased, though it is not as sensitive to changes in the input power. Larger changes may be occurring in the dimerization content as the RF power increases, but as stated previously these lie outside the range of the spectrometer and cannot be observed.

Unlike the neutral spectra, M^+ does not completely dominate the spectrum at high pressures/low power as the peaks positioned at 126 amu and 142 amu are always large peaks in addition to the signal from M^+, as shown in figure 6 b).

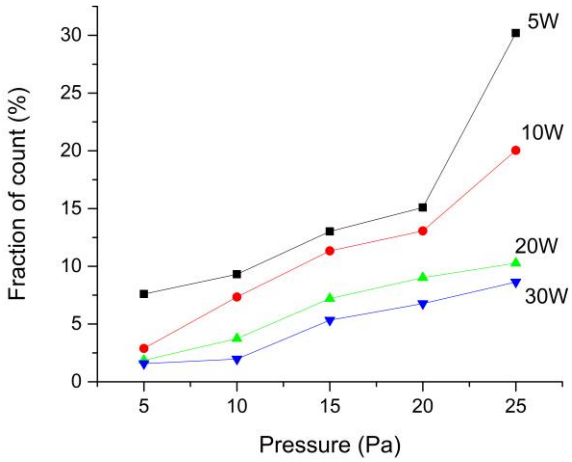

FIG. 7. Percentage of the total ionic mass spectrum signal attributed to the ionised TEMPO molecules, M^+, as the pressure and input power are increased.

The increasing fraction of neutral and ionic species attributed to M or M^+ suggest that in order to preserve the nitroxide properties in the deposited TEMPO plasma polymers the plasma discharge should be operated at higher pressures and lower input powers to

produce highly functionalised films. The average molecular mass, m_{avg}, at each discharge operational pressure and power was calculated using Eq. (4)

$$\boldsymbol{m_{avg}} = \frac{\sum_i \boldsymbol{m_i I_i}}{\sum_i \boldsymbol{I_i}} \qquad (4)$$

where m_i and I_i are the mass and intensity for each signal i in the mass spectrum. Figure 8 shows contour plots of the average mass of species for a) the neutral mass spectra, and b) ionic species. Linear interpolation was used for values between measured data points. The average mass of molecules in the discharge clearly increases at higher pressures and lower input powers. Neutral species appear to have a stronger dependence on the pressure and power than the ions as the average m/z is low for 5 Pa and 10 Pa across the entire power range, and quickly increases as the monomer peak begins to dominate the spectra and dissociation is suppressed at 20-25 Pa for low powers. m_{avg} of ions also increases for low powers and high pressures but is less sensitive as the peaks at 126, 142, and 156 amu make up a significant fraction of the total signal across the pressure and power range used.

The ionic species have a peak around 15 Pa, 5-10 W. As we move to higher pressure, some smaller peaks around 270 amu start to have greater prominence in the mass spectra which implies that under these plasma conditions there may be a significant population of dimers outside the mass range of the mass energy analyser of 300 amu, which were also observed in [26].

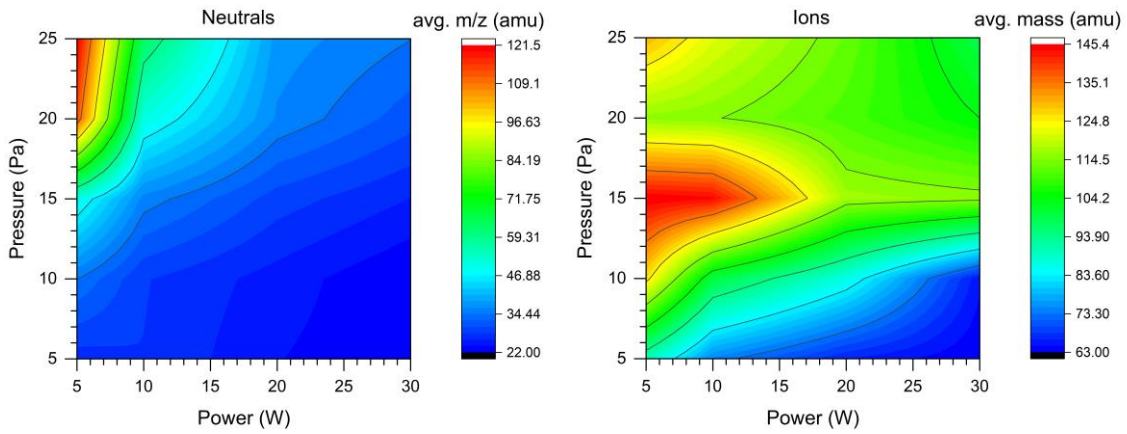

FIG. 8. Contour plots of m_{avg} calculated from the mass spectra data across the pressure and power range investigated for a) neutral species, and b) ions.

C. *Ion Energy Distribution Functions*

1. Effect of Pressure, Fixed Power at 10W

The IEDFs of molecules emerging from the discharge may vary with changing molecular mass as different fragments are produced in different regions of the plasma. Figure 9 shows the IEDFs of the precursor at 156 amu, one high mass molecule at 126 amu, and a lower mass fragment at 58 amu as the operational pressure of the discharge increases with a fixed power at 10W. The first observation is that at lower pressures (5 and 10Pa) all ions, irrespective of m/z have the same energy (= 47 eV, 35.4 eV respectively, taken at centroid of peak). This indicates that the vast majority ions have originated from the plasma bulk and have been accelerated through the full sheath potential drop onto the grounded surface. The large single peak implies that time required for ions to traverse the sheath is much larger than the period of RF oscillation. Ions are accelerated through a DC time averaged potential drop. The small population of low

energy ions at 10 Pa implies that some ions have collided with neutrals as they traversed the sheath. The small secondary peak close to 10 eV is likely slow ions resulting from charge exchange interactions.

As the pressure increases, the IEDFs become broader with a larger contribution from low energy ions as the plasma sheath becomes more collisional, and the sheath potential diminishes with increasing pressure as the observed maximum energy of ions decreases. At 15 Pa, from the high energy tail of IEDF, we can see all ions arrive < 40eV, and this drops < 30 eV at 20 and 25 Pa.

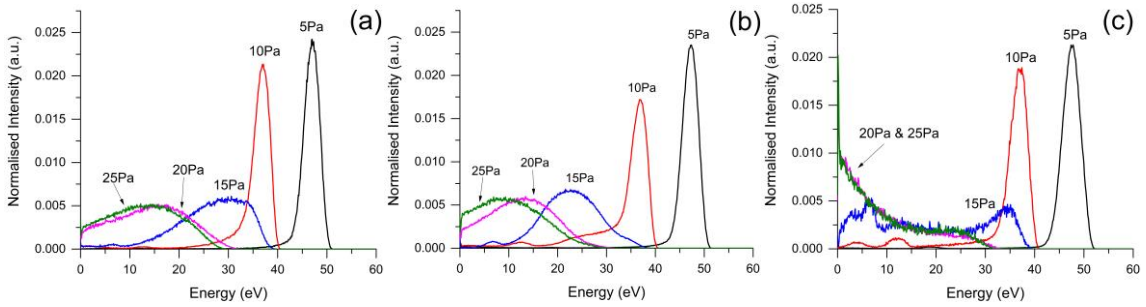

FIG. 9. Normalised IEDF measured across the pressure range investigated for the peaks a) 156 amu, b) 126 amu, and c) 58 amu with a fixed power of 10W.

At ≥ 15 Pa, a disparity emerges between the IEDFs of higher and lower molecular weight particles. IEDFs of lower mass molecules such as 58 amu in figure 10 c), show a more significant low energy population and this suggests a substantial fraction of these molecules have undergone collisions or were formed within the sheath itself. Whilst the IEDF for m/z 156 at 15 Pa shows that a greater portion of these larger ions still originate from beyond the edge of the sheath.

The energy with which ions impact the surface is crucial for determining the likelihood of bond breakage occurring in either the arriving ion or in the polymer films already deposited on the substrate. It is also an important factor for the probability of the molecule subsequently sticking to the surface or sputtering other molecules from the polymer. It has been previously speculated that it is possible to grow polymers from ions that, from a structural perspective, largely remain intact on surface impact [30]: this has been described as "soft landing". [33] It has also been shown experimentally using beams of energy-selected hyperthermal polyatomic ions (monomer = HMDSO, 26 bonds per molecule), the soft landing threshold energy is between 25 -50 eV for the arriving ion [33]. It can therefore be expected (at fixed low power) with changing pressure both a change in the balance of the deposition mode (ions vs radicals) as the ion energy is reduced towards 25eV (or lower), favouring ions, and a much greater retention of the original monomer structure in the final plasma polymer deposit.

2. Fixed Power at 5W

Fig. 10 shows IEDFs for 5 W plasma at the four pressures (5, 10, 20 & 25 Pa): as with 10 W, at 5 Pa all ions arrive with the same energy of 31eV and the distributions are largely collisionless, again with some low energy peaks from slow ions likely due to charge exchange. Unlike 10 W, by 10 Pa all three ions are showing a much more complex IEDFs, where a portion of the ions have undergone collisions before entering the aperture. At 20 and 25 Pa the distributions for m/z 126 & 156 are very collisional with the majority of ions losing energy through collisions in the sheath or originating

from within the sheath itself. A substantial proportion of these ions are arriving at surfaces with energies < 10eV, which would favour the intact soft landing of these ions and has consequences for functional (NO) retention which is discussed in section F.

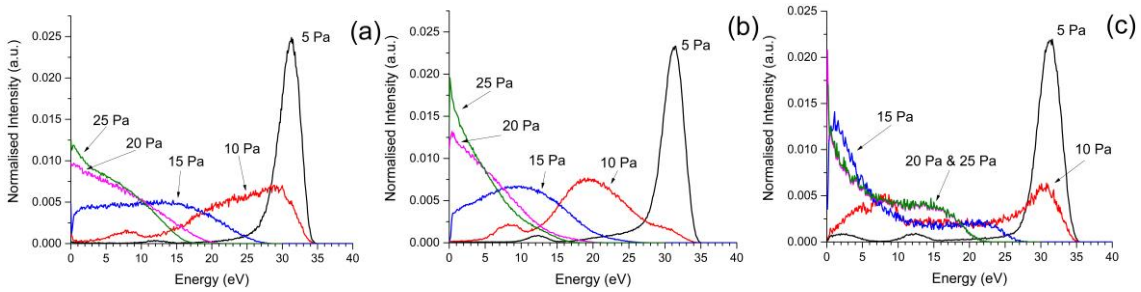

FIG. 10. Normalised IEDF measured across the pressure range investigated for the peaks a) 156 amu, b) 126 amu, and c) 58 amu with a fixed power of 5W.

Due to their larger mass, these molecules can still deposit energy through collisions into substrate atoms with greater efficiency. As a result, at high pressures they are likely to form a more significant contribution to surface radical formation, as well as the generation of other species through processes such as dissociative chemisorption.

D. Deposition Rate Measurements

The QCM was positioned close to the centre of the discharge chamber and estimated the deposition rate of the TEMPO plasma across the investigated discharge conditions. Figure 11 a) shows the changing mass deposition rate per unit area with changing input power for each pressure investigated.

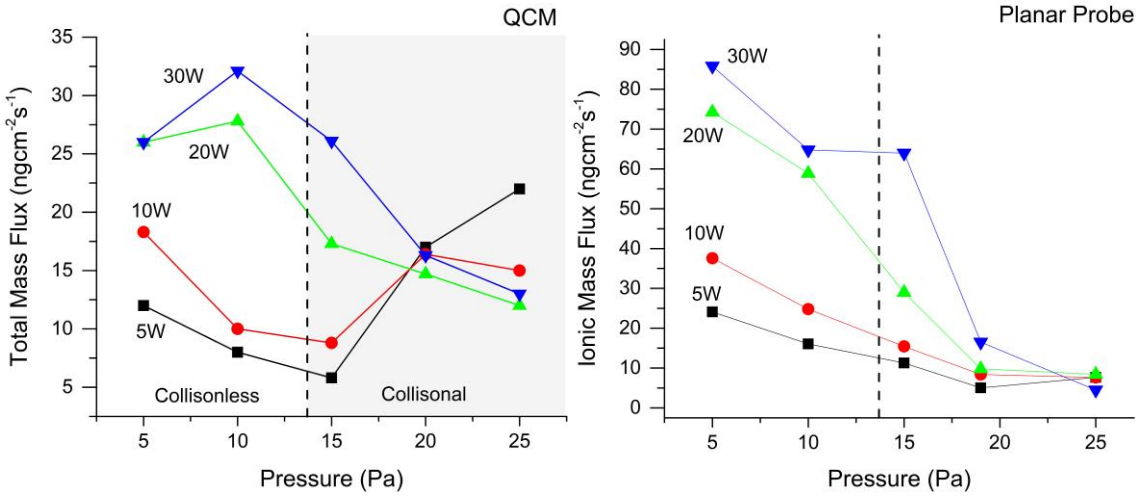

FIG. 11. a) Mass flux rate measured by the QCM and b) ionic mass flux calculated using the heated planar probe data and average ion masses.

The average ion mass was used to calculate an ionic mass flux using the heated electrical probe ion flux measurements, shown in figure 11 b). However the difference between energy distributions at intermediate pressures between certain molecules, such as the TEMPO at 156 amu and the peak of the 58 amu IEDF shown in figures 9 and 10 must be considered. It implies that the mass spectra data may not be entirely representative of the actual positive ion populations in the plasma volume as the mass spectrometer is usually tuned to the maximum signal of the IEDF at 126 amu far from the maximum intensity of the distribution for 58 amu. This will result in an overestimation of the average ion mass and ionic mass flux calculated from the heated probe data.

Figure 11 a) shows that for pressures below 20 Pa the mass deposition rate increases with input power. This is likely due to the greater flux of ions to the grounded quartz surface, as shown by the heated planar probe measurements in figure 2. Fig 11 b shows that,

within the limitations of how the ion mass flux was determined, the total ion mass flux exceeds the total mass deposition rate, with exception of the four data points at high pressure (20, 25 Pa) and the lowest powers (5, 10W).

Ions could themselves directly contribute to the mass of forming polymer or indirectly contribute, as they bombard the surface and create new radical sites, which allow the neutral particle flux to more easily chemisorb onto the forming plasma polymer. The ion sticking probabilities are not known but comparing values at low pressure high power (e.g. 5 Pa & 30 W the ion mass flux exceeds the deposition rate by x3) the sticking probability is likely to be << 1.[6,33] This makes intuitive sense as ions, particularly at higher impact energies will fragment and may sputter surface material.

As the pressure increases the deposition rate generally decreases: the notable exceptions are the data points for high pressure (20, 25 Pa) at the two lowest powers (10, 5 W). Whilst at these four settings the ion mass flux remains relatively constant (Fig 11b) the total mass flux increases. In part F, this observation is brought together with other observations (from MS, IEDFs and XPS) to postulate that the rise in total mass at these data points high pressure / low power might be explained the direct contribution of soft-landing of the intact *M*.

E. X-ray Photoelectron Spectroscopy

TEMPOpp films deposited onto grounded aluminium substrates for 20 minutes were characterised by XPS. Two series of samples were studied; the first series deposited

at a fixed pressure of 15 Pa and powers of 5 – 30 W, while the second series was deposited at a fixed power of 5 W and pressures of 5 – 25 Pa. Wide scans and high resolution C1s, N1s and O1s spectra were recorded for all samples.

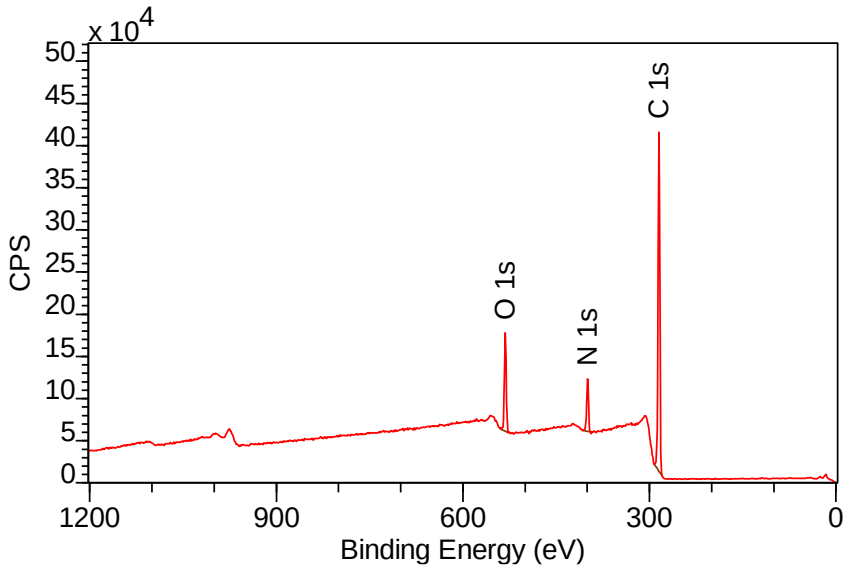

FIG.12. Representative XPS wide scan of a TEMPO pp coating on a grounded aluminium substrate deposited at 5 W, 25 Pa.

Figure 12 shows representative wide scans of TEMPOpp coatings on grounded aluminium substrates. No influence from the substrate could be identified in wide scans for any samples deposited on grounded aluminium substrates, and little or no evidence of contamination could be identified. The atomic composition of TEMPOpp coatings, calculated using experimentally determined sensitivity factors, remains relatively consistent across the range of deposition settings used, with carbon accounting for 69%-71% and nitrogen for 13.5% - 16.0%. Oxygen concentration was observed to vary

slightly more, accounting for 13.1% (5Pa 5W) to 17.3% (15Pa, 30W) of film composition.

1. *Fixed Pressure (=15Pa): Effect of Power*

Figure 13 a shows overlays of C1s and N1s core lines recorded for plasma polymers made at 5, 10, 20 and 30 W, with the C-H/C-C peak corrected to 285 eV. Marked on the overlay are the anticipated positions for six common C environments (C-C/C-H, C-N, C-O, C=O, N-C=O and O-C=O) that were expected to be within the plasma deposits. There are only small changes within the C1s core line over this power range.

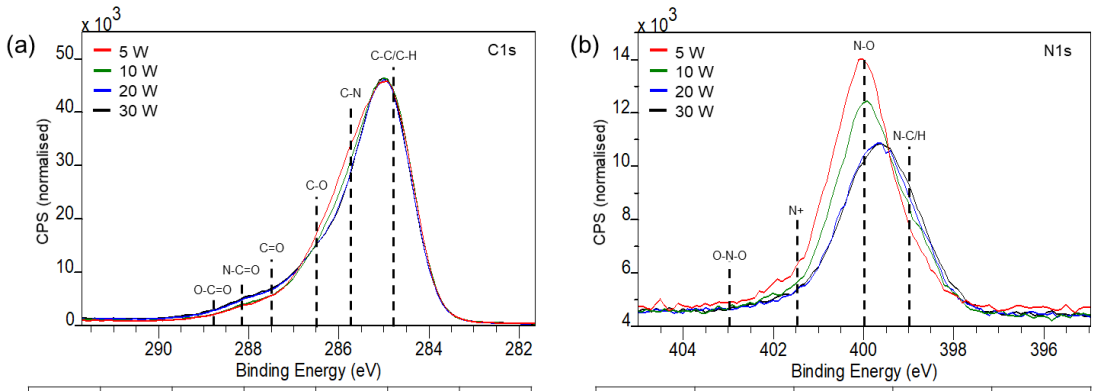

	C-C/H	C-N	C-O	C=O	N-C=O	O-C=O
5 W	45.9%	27.9%	15.2%	6.5%	3.5%	1.0%
10 W	43.5%	30.3%	16.4%	5.9%	3.3%	0.7%
20 W	51.3%	25.0%	14.5%	5.0%	3.2%	0.9%
30 W	53.3%	23.5%	14.3%	4.9%	2.8%	1.2%

	N-C	N-O	N^+	O-N-O
5 W	10.3%	77.5%	10.0%	2.2%
10 W	21.6%	65.1%	10.5%	2.9%
20 W	33.2%	59.3%	5.6%	1.9%
30 W	36.8%	55.1%	6.4%	1.7%

FIG. 13. Overlaid (a) C1s and (b) N1s XPS spectra for effect of power at constant pressure (15Pa). Dotted lines indicate approximate positions of common environments within each envelope.

As power increases a small reduction in C-N is predicted, indicative of ring cleavage and some introduction of new carbon-oxygen environments not in the original starting compound, as C-O, C=O, N-C=O and O-C=O. Oxygen containing environments make up ≤ 30% of the C1s spectra. It should be noted that samples were analysed seven days after creation, meaning a degree of post process oxidation will likely have occurred. The C-N is a potential marker of the intact ring and comparing the fitting of 5 W vs 30 W C-N changes from 27.9% to 23.5% (33.3% would be expected had there been no rearrangement/fragmentation within the TEMPO).

Figure 13b shows effect of power on the N1s core lines. On this overlay three types of N environment are marked, namely, N-C/H, N-O and N^+ that will capture the expected broad classes of N environments. (Within a plasma polymer there will be many similar, yet subtly different N environments that will sit under each of these three types of environment. For example, under the amine there will be primary, secondary and tertiary amines.) A fourth possible environment O-N-O (nitrite) is marked.

From the overlay it can be seen that on going from 5/10 W to 20/30 W there is a loss in N-O, from and an increase in amine i.e. N-C/H. These changes are consistent with loss of O from N-O on going from the monomer to the plasma deposit. This loss of O would not produce any change in C-N in Fig. 13a.

The behaviour identified from overlaying the N1s spectra is supported by peak fitting: a decrease is seen in the N-O component as power increases; at 5W, N-O is 77.5%, while

at 30W it accounts for 55.1%. The N-C/H environment increases substantially in line with power from 10.3% at 5W to 36.8% at 30W.

2. *Fixed Power (=5W): Effect of Pressure*

Figure 14a shows the C1s and N1s core line fits for 5W plasma polymers made at 5 Pa, whilst Fig 14b for 25Pa.

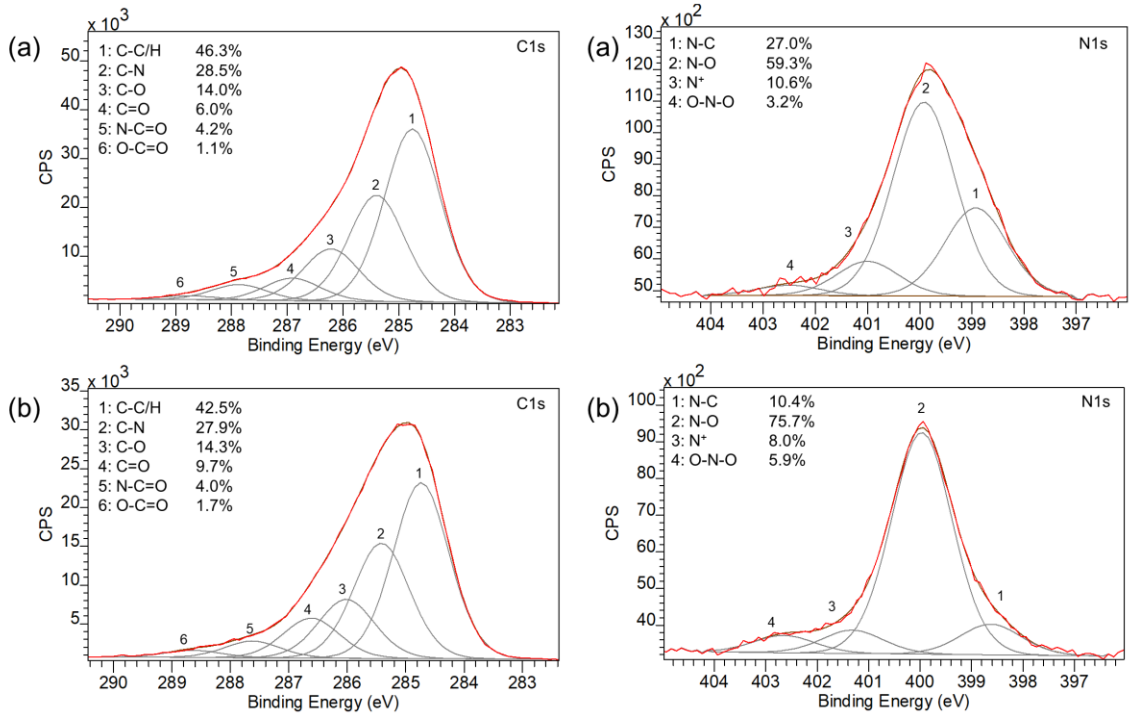

FIG. 14: XPS C1s (left) and N1s (right) high resolution spectra and fits for (a) 5W, 5Pa and (b) 5 W, 25 Pa.

Not much change is seen with pressure in the C-N (28.5% at 5Pa, 27.9% at 25Pa) suggesting that the ring structure is likely to remain intact in the plasma deposits. There is, however, a little bit of additional oxidation at higher Pa.

As with power, the most marked change in pp chemistry occurs with pressure, with a substantially greater retention of N-O at 25 Pa (75.7%) vs. 5Pa (59.3 %), and a corresponding drop in N-C/H from 27.0% at 5Pa to 10.4% at 25Pa. In the 25 Pa pp a fourth peak is evident at 402.8 eV which is assigned to nitrite (NO_2). Whilst appearing in other pps, it is seen most clearly in this low power and high pressure pp.

This finding further supports the evolving hypothesis in recent papers that pressure can be used to further increase functional / structural retention in plasma polymers following a reduction of the plasma power.

F. Retention of N-O and TEMPO Structure

The main purpose of this work is to understand and explain how to retain the nitroxide group and TEMPO structure in plasma polymer deposits. Results suggest the answer is to use a combination of both low power and high pressure to maximise flux of preserved precursor and the retention of the nitroxide group (i.e. within collisional γ-mode). The XPS data has also demonstrated in the case of this experiment that using high pressure in addition to low power leads to greater functional retention.

The explanation for this relies on accounting for how much of the final mass of the polymer arrives from ions, which is difficult. In a single paper and based upon a single compound this would be challenging. However, through the study of many compounds and the following trends have been found consistently [6,20,30,33,34]:

a) High pressure/low power favours an ion flux comprising a large proportion of intact monomer.
b) The IEDF for all ions reduces with pressure; and for the singly charged (protonated) reduces < 25 eV
c) For larger monomers comprising 20+ bonds under this equates to an average ca. 1 eV (or less per bond) and an average of 1eV per bond would not result in breakage. It has been previously argued that ions at ca. 1e V per bond would be "soft landed", which has been demonstrated the point with polyatomic hyperthermal ions[33].
d) Total ion mass fluxes under soft landing conditions are sufficient to explain the entire mass deposition rate

Based on the above we hypothesise that at within γ-mode the deposit grows predominately from intact monomer ions soft landing onto the substrate. Here they impact the surface with low energy, little rearrangement of their molecular structure occurs, and they directly contribute to film growth. Previously this process has also deposited polymer films with little cross linkage in their structure.[33] Gas phase

dimerization may also contribute to polymer growth but cannot be observed due to the limit range of the mass spectrometer.

However, this a simplified view as high pressure/low power conditions will still have multiple other reaction channels occurring within the plasma and at the substrate/polymer surface. It is difficult to speculate on the exact chemistry of the deposited films without further analysis, e.g. using time of flight secondary ion mass spectrometry. However, the importance of these other processes have been “dialled down” and that of ions directly contributing to the mass of deposit has been “dialled up”.

IV. CONCLUSION

In this work the plasma polymerisation of TEMPO across a broad spectrum of input powers and discharge pressures was investigated to study the effect of plasma operating conditions on molecular populations in the discharge volume and the preservation of nitroxide groups in the resulting plasma polymer films. Plasma mass spectrometry and IEDF results have reaffirmed that operating the plasma in a collisional, high pressure regime (γ-mode), or using lower plasma powers, supresses precursor fragmentation in the plasma volume. However, using reduced plasma powers in addition to high operational pressures enhances this effect further, leading to the preserved TEMPO molecule forming an even larger fraction of the total particle flux emerging from the plasma. This is also shown in the XPS analysis of the resulting TEMPO pp films. Films deposited using a low power of 5 W at 5 Pa have a good retention of nitroxides at

59.3%, but a combination of low power and high pressure improves this retention further to 75.7% for 5 W 25 Pa. Maximising the fraction of preserved precursor molecules in the particle flux incident onto surfaces, through high pressure and low plasma powers, has resulted in greater retention of the desired functional group in the deposited plasma polymer film. The results also indicate the mechanism through which ions contribute to the film growth changes in this high pressure, low power regime from the indirect creation of radical sites as they bombard the surface with high energies, to being soft landed on the substrate. Here instead of sputtering and removing material from the polymer film, the preserved precursor ions directly contribute to the film growth. The results of this study have provided insight into the control of plasma polymer deposition in order to maximise retention of the desired functional group and the importance of the ion contribution to the deposition process at lower powers and higher pressures.

ACKNOWLEDGEMENTS

This work was supported by the Engineering and Physical Sciences Research Council (EPSRC), grant numbers EP/S005153/1 and EP/S004505/1.

[1] D. Thiry, S. Konstantinidis, J. Cornil, and R. Snyders, Thin Solid Films **606**, 19 (2016).

[2] L. Detomaso, R. Gristina, G.S. Senesi, R. D'Agostino, and P. Favia, Biomaterials **26**, 3831 (2005).

[3] I. Gancarz, J. Bryjak, G. Poźniak, and W. Tylus, Eur. Polym. J. **39**, 2217 (2003).

[4] A. Cireli, B. Kutlu, and M. Mutlu, J. Appl. Polym. Sci. (2007).

[5] L.M. Watkins, A.F. Lee, J.W.B. Moir, and K. Wilson, ACS Biomater. Sci. Eng. **3**, 88

(2017).

[6] S. Saboohi, B.R. Coad, H.J. Griesser, A. Michelmore, and R.D. Short, Phys. Chem. Chem. Phys. **19**, 5637 (2017).

[7] A. Choukourov, H. Biederman, D. Slavinska, L. Hanley, A. Grinevich, H. Boldyryeva, and A. Mackova, J. Phys. Chem. B **109**, 23086 (2005).

[8] D. Hegemann, E. Körner, and S. Guimond, Plasma Process. Polym. **6**, 246 (2009).

[9] C.L. Rinsch, X. Chen, V. Panchalingam, R.C. Eberhart, J.H. Wang, and R.B. Timmons, Langmuir **12**, 2995 (1996).

[10] A.P. Ameen, R.J. Ward, R.D. Short, G. Beamson, and D. Briggs, Polymer (Guildf). **34**, 1795 (1993).

[11] B.R. Coad, M. Jasieniak, S.S. Griesser, and H.J. Griesser, Surf. Coatings Technol. **233**, 169 (2013).

[12] S. Eufinger, W.J. Van Ooij, and T.H. Ridgway, J. Appl. Polym. Sci. **61**, 1503 (1996).

[13] R.C. Ross and J. Jaklik, J. Appl. Phys. **55**, 3785 (1984).

[14] J. Behnisch, F. Mehdorn, A. Holländer, and H. Zimmermann, Surf. Coatings Technol. **98**, 875 (1998).

[15] F. Truica-Marasescu and M.R. Wertheimer, Plasma Process. Polym. **5**, 44 (2008).

[16] S.A. Voronin, M. Zelzer, C. Fotea, M.R. Alexander, and J.W. Bradley, J. Phys. Chem. B **111**, 3419 (2007).

[17] Q. Chen, R. Förch, and W. Knoll, Chem. Mater. (2004).

[18] L. Denis, P. Marsal, Y. Olivier, T. Godfroid, R. Lazzaroni, M. Hecq, J. Cornil, and R. Snyders, Plasma Process. Polym. **7**, 172 (2010).

[19] S. Fraser, R.D. Short, D. Barton, and J.W. Bradley, J. Phys. Chem. B **106**, 5596 (2002).

[20] S. Saboohi, M. Jasieniak, B.R. Coad, H.J. Griesser, R.D. Short, and A. Michelmore, J. Phys. Chem. B **119**, 15359 (2015).

[21] N. Barraud, M. Kelso, S. Rice, and S. Kjelleberg, Curr. Pharm. Des. **21**, 31 (2014).

[22] S. Korde Choudhari, M. Chaudhary, S. Bagde, A.R. Gadbail, and V. Joshi, World J. Surg. Oncol. **11**, 1 (2013).

[23] W. Wang, Y. Lee, and C.H. Lee, Biotechnol. Adv. **33**, 1685 (2015).

[24] T.D. Michl, J. Barz, C. Giles, M. Haupt, J.H. Henze, J. Mayer, K. Futrega, M.R. Doran, C. Oehr, K. Vasilev, B.R. Coad, and H.J. Griesser, ACS Appl. Nano Mater. **1**, 6587 (2018).

[25] T.D. Michl, D.T.T. Tran, H.F. Kuckling, A. Zhalgasbaikyzy, B. Ivanovská, L.E. González García, R.M. Visalakshan, and K. Vasilev, RSC Adv. **10**, 7368 (2020).

[26] T.D. Michl, D.T.T. Tran, K. Böttle, H.F. Kuckling, A. Zhalgasbaikyzy, B. Ivanovská, A.A. Cavallaro, M.A. Araque Toledo, P.J. Sherman, S.A. Al-Bataineh, and K. Vasilev, Biointerphases **15**, 031015 (2020).

[27] J.D. Whittle, R.D. Short, D.A. Steele, J.W. Bradley, P.M. Bryant, F. Jan, H. Biederman, A.A. Serov, A. Choukurov, A.L. Hook, W.A. Ciridon, G. Ceccone, D. Hegemann, E. Körner, and A. Michelmore, Plasma Process. Polym. **10**, 767 (2013).

[28] A. Morrison and A.P. Davies, Org. Mass Spectrom. **3**, 353 (1970).

[29] L. O'Toole, R.D. Short, A.P. Ameen, and F.R. Jones, J. Chem. Soc. Faraday Trans. **91**, 1363 (1995).

[30] D.B. Haddow, R.M. France, R.D. Short, J.W. Bradley, and D. Barton, Langmuir **16**, 5654 (2000).

[31] A.J. Beck, S. Candan, R.D. Short, A. Goodyear, and N.S.J. Braithwaite, J. Phys. Chem.

B **105**, 5730 (2001).

[32] L. O'Toole, A.J. Beck, A.P. Ameen, F.R. Jones, and R.D. Short, J. Chem. Soc. Faraday Trans. **91**, 3907 (1995).

[33] P.N. Brookes, S. Fraser, R.D. Short, L. Hanley, E. Fuoco, A. Roberts, and S. Hutton, J. Electron Spectros. Relat. Phenomena **121**, 281 (2001).

[34] C. Daunton, L.E. Smith, J.D. Whittle, R.D. Short, D.A. Steele, and A. Michelmore, Plasma Process. Polym. **12**, 817 (2015).